Main Manuscript for

The mouse gut microbiota responds to predator odor and predicts host behavior

Madalena V. F. Real[1,2]*, Maren N. Vitousek[1], Michael J. Sheehan[3], Andrew H. Moeller[1,2]*.

[1] Department of Ecology and Evolutionary Biology, Cornell University, Ithaca, NY 14853, USA.

[2] Department of Ecology and Evolutionary Biology, Princeton University, Princeton, NJ 08544, USA.

[3] Department of Neurobiology and Behavior, Cornell University, Ithaca, NY 14853, USA.

*Madalena V. F. Real and Andrew H. Moeller.

Email: mv469@cornell.edu or andrew.moeller@princeton.edu

Author Contributions: M.V.F.R., Conceptualization, Methodology, Investigation, Formal analysis, Visualization, Writing – original draft, Writing – review & editing; M.N.V., Conceptualization, Methodology, Writing – review & editing; M.J.S., Conceptualization, Methodology, Investigation, Writing – review & editing; A.H.M., Conceptualization, Methodology, Investigation, Formal analysis, Visualization, Writing – original draft, Writing – review & editing, Funding acquisition.

Competing Interest Statement: The authors declare no competing interests.

Abstract

In mammals, chronic stressors can alter gut microbial communities in ways that mediate host stress responses. However, the effects of acute stressors on the gut microbiota, and how these interact with host stress responses, are less well understood. Here, we show that acute exposure of wild-derived mice (*Mus musculus domesticus*) to predator odor altered the composition of the gut microbiota, which in turn predicted host behavior. We experimentally tested the individual and combined effects of brief (15-minute) exposure to synthetic fox fecal odor and prolonged (4-week) social isolation—a well-established chronic stress paradigm. Leveraging behavioral assays, transcriptomics of visceral adipose tissue, and analyses of 3,500 metagenome-assembled genomes (MAGs) generated from our data, we found significant effects of predator odor on host behavior, gene expression, and gut microbiota. Gut microbial communities and host gene expression profiles responded more strongly to brief predator-odor exposure than to prolonged social isolation. The relative abundances of predator odor–responsive bacterial species—including members of the Muribaculaceae and Lachnospiraceae—measured a week after a single predator-odor exposure were associated with host phenotypes assessed the following week, namely grooming and social behaviors and the expression of genes involved in anti-microbial defense, even after accounting for the effects of the stressors. Using random forest classifiers, we found that variation in gut-microbiota composition significantly predicted variation in behavior within treatment groups. These results indicate interactions between the gut microbiota and the responses of wild-derived mice to the threat of predation, and ecologically relevant acute stressor.

Introduction

Animals are faced with diverse stressors that vary in duration and intensity [1-3], giving rise to distinct physiological and behavioral responses [4-7]. In mammals, behavioral [8-11], endocrine [12, 13], and immune [8, 14, 15] stress responses are mediated in part by the community of host-associated microorganisms that reside in the gastrointestinal tract, i.e., the gut microbiota [16], which is shaped by changes in the internal and external host

environment [10, 17-21]. Recent work has shown that chronic stressors, such as social isolation, can alter the gut microbiota in ways that mediate host stress responses [22-27]. In contrast, the effects of acute stressors on the gut microbiota, and the relationships between the gut microbiota and host responses to acute stress, remain less well-understood.

In rodents, the threat of predation represents an intense acute stressor, and animals have evolved to use environmental cues, such as predator-odor marks, to adjust their behavior and avoid predator encounters [28]. Previous work in mice has shown that a single brief exposure to synthetic fox fecal odor 2,5-dihydro-2,4,5-trimethylthiazoline (TMT) can lead to long-lasting behavioral changes, such as increased fearfulness [29-33]. However, the effects of acute exposure to predator odor on the gut microbiota, and the extent to which predator odor–induced changes in the gut microbiota interact with host stress responses, have yet to be investigated.

Here, we tested the effects of acute exposure to predator odor on the gut microbiota, gene expression, and behavior of wild-derived house mice (*Mus musculus domesticus*) and contrasted these effects with those of social isolation, a well-established chronic stress paradigm [21, 22]. We longitudinally sampled the gut microbiota of males and females exposed to predator odor for 15 minutes at the beginning of the third and fourth weeks of the experiment or socially isolated for 4 weeks. These wild-derived mice retain a more diverse gut microbiota than do lab mice and have recently been proposed as a solution to the microbiota-related issues around the poor reproducibility and low translational value of laboratory mouse studies [34, 35]. We found that brief exposure to predator odor had a greater impact on the gut microbiota than did prolonged social isolation. Additionally, the taxonomic composition of the gut microbiota, but not host gene expression profiles, significantly predicted inter-individual variation in host behavior, even after accounting for the effects of the predator-odor treatment. These findings support links between the gut microbiota and host responses to acute stressors.

Results

Predator-odor exposure and social isolation gave rise to stress-associated behaviors

We compared the effects of brief exposure to predator odor to those of prolonged exposure to a social isolation—a well-established chronic stress model. All experiments were conducted using wild-derived mice originally captured in Saratoga Springs (New York, USA) in 2012 and since inbred in the lab [36-38]. At the beginning of the experiment (D0), we separated groups of 6-week-old same-sex littermates into pair- and single-housed mice (Figure 1A). Two weeks later (D15), we exposed these mice to 35 µL of either synthetic fox fecal odor (2,5-dihydro-2,4,5-trimethylthiazoline, TMT) or a control scent (deionized water, H_2O) for 15 minutes. We repeated this exposure procedure the following week (D22). The full factorial design produced 9 unstressed control cages (10 male and 8 female pair-housed H_2O-exposed mice), 6 predator-odor cages (6 male and 6 female pair-housed TMT-exposed mice), 8 social-isolation cages (3 male and 5 female single-housed H_2O-exposed mice), and 9 cages that experienced both stressors (4 male and 5 female single-housed TMT-exposed mice; Dataset S1).

We assessed whether brief predator-odor exposure and prolonged social isolation acted as stressors in wild-derived mice by examining the effects of these treatments on host behavior with linear mixed-effects models (LMM) that accounted for sex, litter, and cage effects (Figure 1B; Table S1 and S2). We found that both stressors increased fearfulness in wild-derived mice, as both TMT-exposed (LMM p-value = 0.022) and socially isolated mice (LMM p-value = 0.048) displayed significantly reduced occupancy of the exposed central area during the open field test [39]. Mice individually exposed to TMT (pairwise LMM p-value = 0.015) or socially isolated (pairwise LMM p-value = 0.041) were significantly more fearful (i.e., displayed reduced center occupancy) than unstressed controls, while mice that experienced both stressors displayed a non-significant trend toward increased fearfulness (pairwise LMM p-value = 0.067). There were no significant differences in overall locomotion between the treatment groups (predator odor: LMM p-value = 0.257; social isolation: LMM p-value = 0.588). These results confirm that, in line with previous work in lab mouse strains [4, 22, 40], predator-odor exposure and social

isolation functioned as stressors that increased fear-associated behaviors in wild-derived mice.

Predator-odor exposure has also been shown to lead to a reduction in self-grooming [32], which is part of a suite of behaviors that are inhibited when rodents enter a more vigilant state after the threat of predation [41]. We assessed grooming behavior with the splash test [42], where individual mice were sprayed with a palatable sucrose solution and their grooming behavior was measured for 5 minutes. We observed that social isolation, but not predator-odor exposure, significantly decreased grooming behavior (LLM p-value = 0.035), such that both socially isolated mice (pairwise LLM p-value = 0.029) and mice that experienced both stressors (pairwise LLM p-value = 0.039) spent significantly less time grooming than did unstressed controls (Figure 1B).

Both brief predator-odor exposure [43] and prolonged social isolation [22, 40] have been previously reported to decrease rodent sociability, here measured by the relative time spent interacting with a social stimulus (stranger) *versus* a non-social stimulus (empty cup) in the three-chamber test [44]. Contrary to prior work in lab mice [43], we found that pair-housed wild-derived mice exposed to predator odor displayed increased sociability, spending significantly more time interacting with the social stimulus than the non-social stimulus (paired Wilcoxon test p-value = 0.002; Figure S1) and displaying a social preference index significantly greater than zero (one-sample t-test p-value = 0.001; Figure 1B). Interestingly, the social preference of pair-housed mice exposed to TMT was significantly higher than that of their single-housed counterparts (pairwise LMM p-value = 0.009). We did not observe significant sex differences in any of the assayed behaviors (LLM p-values > 0.05). Overall, our results show that both brief exposure to predator odor and prolonged social isolation resulted in an increase in stress-related behaviors of wild-derived mice (i.e., fearfulness and, in the case of socially isolated mice, reduced self-grooming), and that predator-odor exposure in the context of pair housing increased sociability.

Predator-odor exposure altered the transcriptome of an endocrine and immunological tissue

Given the observed effects of brief exposure to predator odor and prolonged social isolation on the behaviors of wild-derived mice, we next investigated the impacts of these stressors on gene expression profiles in the visceral adipose tissue (VAT). The VAT can function as an endocrine organ, secreting adipokine hormones that protect against the development of depressive- and anxiety-like phenotypes after chronic stress and regulate negative feedback on the HPA axis [45]. The VAT also has important immune functions, harboring several immune cells and secreting pro- and anti-inflammatory cytokines [46, 47]. Both acute and chronic stress have been shown to increase gut permeability, leading to the translocation of microbes and their metabolites from the gut lumen to surrounding tissues [48]. The VAT can detect these microbial signals [49] and inhibit bacterial infection, systemic inflammation, and sepsis [50, 51] through, for example, the secretion of anti-microbial peptides (AMPs) [52, 53]. Increased inflammation in the VAT has also been shown to impact mouse behavior [54]. To investigate the interactions among this immune-endocrine organ, mouse stress responses, and the gut microbiota, we used 3' RNA-seq to sequence the VAT transcriptomes of mice dissected at the end of the experiment (D33). In total, 35 samples met our quality threshold of over 1 million transcripts/sample, averaging 6.54 million (SD = 3.22 million) transcripts/sample (Dataset S2).

We found that TMT exposure, but not social isolation, significantly altered the VAT gene expression profile (PERMANOVA of Euclidean distances accounting for sex and litter; predator odor: p-value = 0.035; R^2 = 0.047; social isolation: p-value = 0.097; R^2 = 0.037; Figure S2; Table S3). We tested for differentially expressed genes (DEGs) between mice exposed to individual stressors and unstressed controls. We found that, compared to social isolation, predator odor led to a greater number of DEGs (absolute $\log_2$(fold change) (LFC) > 1 and FDR-adjusted p-value < 0.01; Figure 1D; Dataset S3) and a larger mean fold-change in gene expression (Wilcoxon test p-value = 0.026; Figure S3). Interestingly, these DEGs were significantly enriched in biological pathways related to anti-microbial humoral immune responses, including those mediated by anti-microbial peptides (AMPs; FDR-adjusted p-value = 0.007; Figure 1E; Table S4). These results show that brief

predator-odor exposure had a greater impact on VAT gene expression than did prolonged social isolation.

Predator-odor exposure had a greater impact on the gut microbiota than did social isolation

We assessed the impacts of brief exposure to predator odor and prolonged social isolation on the gut microbiota by sequencing the metagenomes of fecal samples collected at the beginning (D0) of the experiment, immediately before the TMT exposures (D15 and D22), and the end of the experiment (D30; Figure 1A; Dataset S4A). Sequencing D0 and D30 samples yielded a mean of 33.6 million (SD = 5.0 million) reads/sample. Intermediate samples from D15 and D22 were sequenced at lower depth, yielding a mean of 10.0 million (SD = 2.4 million) reads/sample. We assembled and binned D0 and D30 reads into metagenome-assembled genomes (MAGs) using a custom automated workflow (MAGmaker), following previously published methods [55]. The MAGmaker workflow yielded 6,404 MAGs, 3,542 of which were high quality (>90% completeness, <5% contamination). We then created a custom database of representative species-level genome bins (SGBs) by dereplicating high-quality MAGs at 95% average nucleotide identity (ANI). SGBs were classified with the Genome Taxonomy Database [56, 57] (Dataset S4B), and their relative abundances in all samples were quantified using InStrain [58] (Dataset S4C). The mean mappability of our samples to the SGBs was 75.75% (SD = 3.04%), indicating that the custom-made SGB database was generally representative of the bacterial diversity in our samples. Samples were rarefied to the minimum library size before beta-diversity analyses (8,470,661 reads for D0 and D30 samples, and 3,896,354 reads for D15 and D22 samples; Dataset S4D).

We tested the effects of predator-odor exposure and social isolation on the SGB profile through PERMANOVA analyses of Jaccard and Bray-Curtis dissimilarities, accounting for sex, litter, and cage effects. In contrast with previous findings that 4 weeks of social isolation altered the gut microbiota of male lab mice [22, 23], social isolation had no effect on mean SGB composition at D30 (Table 1; Figure 1C). Instead, social isolation only significantly affected Bray-Curtis dissimilarities at D22 (Table 1). We did, however,

find that social isolation significantly increased the inter-host variance in the SGB composition at D30 (Jaccard PERMDISP *p*-value = 0.033), and socially isolated mice displayed significantly higher SGB turnover relative to pair-housed mice, as measured by the intra-individual Jaccard dissimilarity between the beginning (D0) and end (D30) of the experiment (LMM social isolation: *p*-value = 0.025; predator odor: *p*-value = 0.427; Figure S4). In contrast, TMT exposure did not significantly change the inter-individual variance in SGB profiles (Jaccard PERMDISP *p*-value = 0.177) but instead significantly shifted the mean SGB composition (Jaccard PERMANOVA *p*-value = 0.016). This difference was not observed before predator-odor exposure at D0 and D15 (Table 1). Thus, predator-odor exposure drove a significant shift in the SGB profile of male and female mice sampled one week after the second TMT exposure (D30; Table 1; Figure 1C). Overall, these results indicate that two acute exposures to TMT were sufficient to shift the SGB profiles of the mouse gut microbiota, that this effect was maintained for at least one week, and that the impacts of predator-odor exposure on gut-microbiota composition were greater than those of chronic social isolation.

Predator-odor exposure drove persistent alterations in the relative abundances of specific SGBs

Given the observed changes in gut-microbiota composition following predator-odor exposure, we next investigated which specific microbial taxa drove these patterns. We found that a single exposure to TMT was sufficient to significantly alter the relative abundances of several SGBs (D22 absolute LFC > 1 and FDR-adjusted *p*-value < 0.01; Figure 2A; Dataset S5). Seven of these SGBs remained differentially abundant (DA) one week after the second TMT exposure at D30 (Table 2). These results demonstrate that a subset of SGBs in the gut microbiota of wild-derived mice displayed persistent responses to brief predator-odor exposure and prolonged social isolation.

Predator odor–responsive SGBs co-varied with host anti-microbial and behavioral responses

As predator-odor exposure up-regulated the expression of genes involved in AMP production, we investigated possible associations between the expression of these AMP-associated genes and the relative abundances of microbes that responded persistently to TMT exposure (DA at both D22 and D30) (Figure 3). We controlled for the effects of the stressor treatments (Pair H_2O, Pair TMT, Single H_2O, Single TMT) by testing these associations using partial Spearman correlations, that residualized the AMPs expression levels and the relative abundances of SGBs against the treatment group. We found that, a week after the first TMT exposure (D22), the relative abundances of SGB051—identified as Muribaculaceae species *Lepagella* sp. 002361155 and depleted in TMT-exposed mice—and the relative abundances of TMT-responsive SGB105 and SGB107—identified as Lachnospiraceae species *Acetatifactor* sp. 011959105 and Borkfalkiaceae species *Gallimonas* sp. 910585595, respectively—were negatively associated with all genes involved in AMP production (Spearman's Rho < 0; FDR-adjusted *p*-value < 0.05). The relative abundances at D22 of all other TMT-responsive SGBs showed positive associations with genes involved in AMP production, although, after correcting for multiple testing, this correlation was only significant for SGB074—identified as Oscillospiraceae species *Pelethomonas* sp. 009774055. These results show that, independent of the effects of stressor treatment, the relative abundances of predator odor–responsive SGBs were significantly associated with host AMP gene expression.

We also tested whether the relative abundances of predator odor–responsive SGBs co-varied with host behavioral responses independently of the effects of stressor treatment (Figure 3). We found that the D22 relative abundances of all predator odor–responsive SGBs but one were negatively associated with mouse social preference. Lachnospiraceae members SGB158 and SGB105, which were enriched in TMT-exposed mice, were also negatively associated with grooming behavior. These findings indicate that behavioral responses to predator-odor exposure, such as reduced grooming and social preference (particularly for single-housed mice exposed to TMT), could be partially explained by the relative abundances of TMT-responsive SGBs measured a week prior.

The gut microbiota was a better predictor of host behavior than was host VAT gene expression

Motivated by the observation that host phenotypes could be partially explained by the relative abundances of specific predator odor–responsive SGBs, we tested the predictive power of the entire gut microbiota. To this end, we trained a random forest model residualized against stressor treatment to predict host behavior based on SGB relative abundances at each timepoint. We tested whether inter-individual variation in the gut microbiota significantly predicted variation host behavior within treatment groups (Pair H_2O, Pair TMT, Single H_2O, Single TMT). This analysis asked whether, after accounting for the effects of stressor treatment, gut microbiota composition predicted future mouse behavior. The model's performance was assessed through a 5-fold cross-validation strategy, and we conducted a permutation test to measure the statistical significance of the observed R^2 values. We found that inter-individual variation in SGB relative abundances at D30 significantly predicted grooming behavior (Permutation test *p*-value = 0.016 and R^2 = 0.021; linear regression *p*-value = 0.0195) and social preference (Permutation test *p*-value = 0.001 and R^2 = 0.102; linear regression *p*-value = 0.0324), but not fearfulness (i.e., center occupancy; Figure 4A; Table S5). SGB relative abundances at D0, D15, or D22 were not predictive of behavior (Table S5). Of the SGBs we found to respond persistently to predator-odor exposure (DA at both D22 and D30), SGB107 and SGB158 ranked among the top half most important features for predicting grooming and social behavior (Figure 4B; Table S6). SGB105 and SGB002 were also important predictors of social preference, with the latter—identified as Rikenellaceae species *Alistipes* sp. 910587675—ranking in 20th place. Furthermore, we found that the gut microbiota was a better predictor of host behavior than was VAT gene expression, which did not significantly predict behavioral phenotypes (Permutation test *p*-value > 0.1 and $R^2 < 0$; Figure 4A; Table S5). These results indicate that the gut microbiota sampled at the end of the experiment, a week after the second TMT exposure, significantly predicted host behavioral phenotypes measured days later.

Discussion

We found that exposure of wild-derived mice to an acute stressor—predator odor—promoted stress-associated behaviors, altered gene expression patterns in the visceral adipose tissue through the activation of the AMP-mediated anti-microbial responses, and shifted the species composition of the gut microbiota. Surprisingly, we found that brief exposure to predator odor had a larger impact on the VAT transcriptome and the gut microbiota SGB profile than did prolonged social isolation—a well-established chronic stress model previously shown to impact the gut microbiota [22, 23]. Moreover, variation in gut-microbiota composition at the end of the experiment (D30) predicted host behaviors within treatment groups (i.e., after accounting for the stressor effects). These results show that predator odor alters the murine gut microbiota and suggest links between inter-individual variation in the gut microbiota and behavioral responses in the context of predation stress.

By comparing the effects of two distinct stressors and their combination on the gut microbiota, host gene expression, and behavior, our study builds on prior work that focused on the effects of individual stressors [22, 23, 59, 60]. We observed that the combination of stressors often had non-additive effects, exemplifying the context dependence of the stress response [4]. For example, we observed that pair-housed mice exposed to predator odor displayed significantly higher social preference than did their socially isolated counterparts, demonstrating that the social environment can affect the response to consequent stressors. In our case, pair-housed mice might seek out proximity with conspecifics when under the threat of predation—a behavior described as huddling [61]—while single-housed mice exposed to predator odor display the asocial behavior commonly observed after chronic stressor exposure [62].

We identified both general and stressor-specific responses in hosts and their gut microbiota. For example, we observed that both stressors increased the expression of AMPs in the VAT. Interestingly, the expression of these AMPs co-varied with the relative abundances of several stressor-responsive taxa, even after accounting for stressor effects (Figure 3). For example, SGB051, which was depleted in TMT-exposed mice, was negatively associated with all genes involved in AMP production. This SGB was identified

as a Muribaculaceae, a family that has been associated with anti-inflammatory markers [63-65] and found to be depleted in inflammatory bowel disease (IBD) [63, 66, 67]. Muribaculaceae produce short-chain fatty acids (SCFAs), which have been shown to stimulate mucus production and reduce inflammation [68], and members of this family also engage in cross-feeding behavior with known probiotic bacteria, such as *Bifidobacterium* and *Lactobacillus* [69]. The associations observed in our study could be due to either SGB051 growing better in the absence of AMPs or to a negative effect of this species on anti-microbial responses. One possible explanation for our results is that responses of the gut microbiota to predator odor were mediated by VAT inflammation triggered during the acute stress response. Alternatively, it is also possible that predator-odor exposure led to changes in the gut microbiota that triggered VAT inflammation. Given that both increased VAT inflammation [54] and stress-induced changes in the gut microbiota [22-24] have been previously shown to affect mouse behavior, the observed behavioral effects of stressor exposure may be mediated by signaling along the gut-brain-immune axis [70-72]. Alternatively, the gut microbiota may interact with host behavior in a VAT-independent manner, as variation in gut species composition was a better predictor of mouse sociability and grooming behavior than was the VAT gene expression profile. Understanding the mechanisms underlying the associations between the predation stress–altered microbiota, host inflammatory responses, and behavior will require controlled experiments in germ-free animals designed to test the effects of stressor-associated microbiota on mouse phenotypes that can complement previous work showing that host responses to acute stressors are microbiota-dependent [73-76].

Several results contradicted expectations based on previous literature using lab mouse strains. For example, while 4 weeks of social isolation was sufficient to alter the gut microbiota of C57BL6 males [22, 23], in our study only predator-odor exposure significantly altered the species composition of the gut microbiota. This discrepancy could be due to differences in the robustness of the gut community to perturbation, as lab mouse strains have a depleted, and potentially more volatile, gut microbiota compared to wild mice [34, 35]. Previous work has shown that wild-derived mouse lines can retain microbiota from wild populations for over a dozen generations in the lab [77]. Additionally,

there is evidence that wild-derived mice are less sociable than lab mouse strains [78-80], potentially increasing their tolerance for social isolation. This hypothesis is supported by our observation that unstressed controls lack a clear social preference, whereas commonly used lab strains tend to display high sociability [81]. The significant social preference displayed by pair-housed mice exposed to predator odor similarly contradicts previous results in the literature [43]. Brief predator-odor exposure is likely also a more potent stressor for wild-derived mice than prolonged social isolation. This is supported by previous work showing wild-derived mice are more readily responsive to the threat of predation (e.g., higher freezing and flight) than lab mice [82]. Thus, this work adds to a growing body of evidence motivating the incorporation of wild-derived mice into research as a biologically relevant complement to the work conducted on classic lab strains [34, 35, 78, 83].

Materials and Methods

All procedures conformed to guidelines established by the U.S. National Institutes of Health and have been approved by the Cornell University Institutional Animal Care and Use Committee (protocol #2015-0060).

Animals

We used a wild-derived *M. m. domesticus* line, NY3, which was captured in Saratoga Springs (NY, USA) in 2012 and inbred in captivity [36-38]. These mice are related to the SAR/NachJ lines currently provided by the Jackson Laboratory [83]. Mice were kept on an inverted light cycle (light:10pm-10am) and all handling was conducted during the active (dark) phase using red light. Standard chow diet and water were available *ad libitum*.

Stressor Treatments

Social Isolation

Mice were weaned at 3 weeks of age (M = 22 days old, SD = 2) and co-housed with same-sex littermates. At 6 weeks of age (D0, mice were M = 37 days old, SD = 8), we separated

co-housed same-sex littermates into pair- and single-housed mice, in a total of 8 male and 7 female mouse pairs, and 7 male and 10 female mice that were socially isolated.

Predator-Odor Exposure

Two weeks after the start of the experiment (D15; mice were M = 57 days old, SD = 5), we exposed mice to synthetic fox fecal odor, 2,5-dihydro-2,4,5-trimethylthiazoline (TMT) (90% purity; BioSRQ, Sarasota, FL, USA). Mice were individually placed in an empty cage, brought to a fume hood, and a filter paper with 35 µL of either TMT or deionized water (H_2O) was placed on their cage metal grid topper for 15 minutes. After the exposure period, we removed the filter paper, keeping the mice in the fume hood for an additional 15 minutes to ensure the TMT was removed from the work area. Afterwards, all mice were returned to their home cages. We exposed control mice first and the TMT-treated mice last, to ensure controls never encountered the predator odor. We repeated this exposure procedure the following week (D22; mice were M = 64 days old, SD = 5). In total, 10 males and 11 females were exposed to TMT, while 13 males and 13 females were exposed to H_2O. Considering both stressors, there were 9 pair-housed H_2O-exposed cages (5 male pairs and 4 female pairs), 6 pair-housed TMT-exposed cages (3 male pairs and 3 female pairs), 8 single-housed H_2O-exposed cages (3 males and 5 females), and 9 single-housed TMT-exposed cages (4 males and 5 females).

Behavioral Assays

We assayed mouse behavior on the fifth week of the experiment (D30; mice were M = 72 days old, SD = 6), over three consecutive days. The tests were ordered from least to most disruptive, starting with the Open Field Test (OFT) [39], followed by the Splash Test (SP) [42], and ending with the Three-Chamber Test (3CT). All behavior trials were conducted between 1:00-6:00 pm, and as mice were kept on an inverted light cycle, this time corresponded to the animals' active (dark) phase. The OFT and 3CT were conducted inside a soundproof chamber in a separate behavior room. The mice were habituated to the behavior room for at least 30 minutes. We alternated the testing order between experimental groups and wiped the behavioral apparatuses between trials with 70%

ethanol. An infrared camera placed above the apparatuses recorded the behavior tests. All analyses were conducted by the same experimenter, who was blind to the experimental condition.

Open Field Test

Mice were placed in the center of a white PVC arena (48 × 46 × 44 cm) and allowed to explore for 10 minutes. We used ToxTrac [84] to detect mouse trajectories and calculate total distance walked and time spent in the center of the arena (34 × 32 cm; ½ of the area). After the test, each mouse was housed in a new individual home cage.

Splash Test

Our protocol was adapted from Nollet (85). On the second day of behavior tests, each mouse was placed in an empty "spray" cage and sprayed on their dorsal coat with a 10% sucrose solution. Mice were then quickly returned to their home cage, and grooming behavior was measured for the following 5 minutes. We directly measured the duration of the grooming behavior by using a chronometer to time observed instances of nose/face grooming, head washing, and body grooming, as described by Kalueff and Tuohimaa (86).

Three-Chamber Test

Mice were placed in the middle chamber of a transparent plexiglass three-chamber arena for a 5-minute habituation period. We then placed overturned wire cups on diagonally opposite corners of each side chamber. One of the cups was empty (non-social stimulus), while the other contained a stranger mouse of the same sex as the test mouse (social stimulus). The position of the stimuli was counterbalanced between trials. We allowed the test mouse to explore the arena for 10 minutes. The recorded video footage was manually scored with BORIS where we logged interactions with the social and non-social stimuli following recommendations by Rein, Ma (44). These were behaviors such as directly interacting with the stranger mouse between the cup's wire bars and/or sniffing the cup or any protruding part of the stranger mouse (e.g., tail). Climbing on top of the cups or grooming in their proximity was not counted as an interaction. Additionally, we calculated

the social preference index, which is the difference in interaction time between the social and non-social stimulus, normalized by the total time interacting with both stimuli [44]. Significantly higher interaction time with the social *versus* non-social stimulus was interpreted as the existence of a social preference [44].

Host Gene Expression

Tissue Collection and Gross Morphometry

Mice were humanely euthanized with an overdose of CO_2 followed by cervical dislocation. Immediately after, we measured body mass and length (nose-tip to tail-base) and dissected the visceral adipose tissue (VAT), which was flash frozen and stored at -80°C.

Transcriptomic Sequencing

Total RNA was extracted from the VAT using the RNeasy Lipid Tissue Mini Kit (Qiagen, Germantown, MD, USA). Briefly, approximately 50 mg of VAT were placed in Bead Ruptor 2 mL tubes with 2.4 mm metal beads (Omni International, Kennesaw, GA, USA) and 1 mL of QIAzol Lysis Reagent (Qiagen). The tissues were homogenized with a Bead Ruptor (Omni International) at speed 5 for 30 s. We followed the manufacturer's instructions for the remainder of both RNeasy protocols, including the optional drying step of placing the RNeasy spin column in a new 2 mL collection tube and centrifuging at full speed for 1 minute. Total RNA was eluted twice in 30 µL of RNase-free water (Qiagen). We assessed the concentration and purity of the extracted RNA with a NanoDrop Microvolume Spectrophotometer (Thermo Fisher Scientific) for all samples and with a TapeStation (Agilent Technologies, Santa Clara, CA, USA) for 10% of the samples. The 3'RNA-seq libraries were prepared at Cornell University's Biotechnology Resource Center (BRC; Ithaca, NY, USA) and sequenced on a NextSeq 500 (Illumina).

Transcriptomic Data Processing

We assessed the quality of our transcriptomic data with FastQC (v0.72.0) [87] and filtered out samples with less than 1 million reads. The remaining transcripts were aligned against the *Mus musculus* reference genome (GRCm39 GCF_000001635.27) using STAR

(v2.7.10b; setting: --quantMode GeneCounts --outSAMtype BAM SortedByCoordinate) [88].

Gut Microbiota

Fecal Collections

We sequenced the metagenome from fecal samples collected at the beginning of the first (D0), third (D15), fourth (D22), and fifth (D30) weeks of the experiment. D15 and D22 samples were collected immediately before the predator-odor exposure procedure. D30 samples were collected immediately before the first behavioral assay. All fecal samples were flash frozen and stored at -80°C.

DNA Sequencing

Total microbial DNA was extracted with the Quick-DNA MagBead extraction kit (Zymo, Irvine, CA, USA) using an OT-2 liquid handling robot (Opentrons, New York, NY, USA). The metagenomic libraries were prepared with the TruSeq kit (Illumina, San Diego, CA, USA) at Cornell's BRC. The D0 and D30 libraries were sequenced in a NovaSeq 6000 S4 (PE150 bp; Illumina) at the UC Davis Genome Center (Davis, CA, USA), while the D15 and D22 libraries were sequenced in a NovaSeq X (2 × 150 bp; Illumina) at Cornell's BRC.

Metagenomic Data Processing and Analysis

We processed our metagenomic samples and assembled MAGs using a custom snakemake [89] workflow (MAGmaker) [55]. Briefly, sequencing adapters were trimmed with Cutadapt (v17.4; setting: "-a AGATCGGAAGAGCACACGTCTGAACTCCAGTCA -A AGATCGGAAGAGCGTCGTGTAGGGAAAGAGTGT -a GGGGGGGGGGGGGGGGGGGG -A GGGGGGGGGGGGGGGGGGGG -u 10 -U 10 --minimum-length 1 --nextseq-trim 20") [90], host reads removed with Bowtie2 (v2.5.1; setting: "--very-fast"; host reference genome: GRCm39 GCF_000001635.27) [91], and the quality of our metagenomic data was assessed with FastQC (v0.72.0) [87]. We assembled high-quality non-host reads from D0 and D30 into contiguous sequences (contigs) using Megahit (v1.2.9) [92] and assessed assembly quality with Quast (v5.2.0) [93]. We then

calculated the distances between our samples using SourMash (v4.4.0) [94] and selected the 11 samples most dissimilar to all others to be used as "prototypes" against which the metagenomic reads from all samples were mapped with Minimap2 (v2.24) [95]. The resulting coverage information was input into three different binning algorithms: CONCOCT (v0.4.2) [96], MetaBAT2 (v2.15) [97], and MaxBin (v2.2) [98]. We then used DASTool (v1.1.6) [99] to select the optimal set of bins among the three binners. The resulting MAGs were quality controlled for completeness and contamination with CheckM (v1.2.2) [100] and GUNC (v1.0.6) [101]. We created a custom genome database by dereplicating high-quality MAGs (>90% completeness, <5% contamination) into 95% average nucleotide identity (ANI) species-genome bins (SGBs) using dRep (v3.4.2) [102]. We profiled these SGBs using GTDB-Tk (v2.4.0) [57]. Finally, we calculated the relative abundances of representative SGBs in our samples by mapping all metagenomic reads against our custom genome database with Bowtie2 and profiling them using InStrain (v1.8.0) [58]. The counts from our mapped reads were normalized by the genome size of the representative SGB the read mapped to and the library size of the metagenomic sample from which the read originated. We then converted these normalized counts into a relative abundances percentage. The Jaccard and Bray-Curtis dissimilarities between samples were calculated with phyloseq (v1.42.0) [103].

Statistical Analyses

All data analyses, except were indicated, were conducted in R (v4.2.2). Means are reported alongside standard deviations (SD). Linear mixed-effects models, controlling for litter and cage as a random effect, were implemented via lmerTest (v3.1) [104]. We tested which factors explained the microbiota dissimilarity matrix by running a PERMANOVA [105] via adonis2 and a PERMDISP [106] via betadisper, both included in vegan (v2.6) [107]. We calculated normalized counts and differential gene expression or taxa relative abundances between stressor treatments using DESeq2 (v1.42.1) [108] with LFC shrinkage using the "ashr" adaptive shrinkage estimator [109], after filtering for genes or taxa with one or more counts in at least three samples. We identified biologically meaningful pathways within DEGs with a biological pathway enrichment analysis using clusterProfiler

(v4.10.1) [110, 111]. We investigated whether species relative abundances significantly explained variation in behavior while controlling for stressor treatment effects with a random forest model implemented via Python's scikit-learn (v1.6) [112]. We evaluated our model's performance using a 5-fold cross-validation strategy, where we subset our data into 5 different "folds" and trained the model 5 times, using 4 of the folds as the training data and the remaining fold as the test data. Our performance metric (R^2) was averaged across all 5 iterations. This way, each data point is used at least once to both train and test our model, and the R^2 reflects the model's performance across the entire dataset. We evaluated the statistical significance of the R^2 using a permutation test, where we randomized the associations between behavior and species relative abundances and recalculated R^2 for 1000 iterations, thus generating a distribution of R^2 values expected under the null hypothesis that behavior is not associated with species relative abundances. We calculated a *p*-value by measuring the likelihood of observing the R^2 resultant from our random forest in the null distribution. Lastly, we assessed the importance of individual SGBs in predicting behavior using Python's scikit-learn (v1.6) [112]. Throughout the analyses, a *p*-value < 0.05 was considered statistically significant, except where otherwise indicated. All plots were created with ggplot2 (v3.4.1) [113]. All figure panels were assembled using Inkscape 1.2.

Acknowledgments

Funding was provided by the National Institutes of Health (NIH) grants R35 GM138284 and R01 DK139214 to A.H.M. NIH had no role in study design, data collection, and interpretation, or the decision to submit the work for publication. The authors declare no competing interests.

We acknowledge Cornell's Biotechnology Resource Center for the help with sequencing host transcriptomic and fecal metagenomic data. We also thank Sylvia Bayrakdarian for her help with the animal care and behavioral tests.

References

1. Romero LM, Dickens MJ, Cyr NE. The Reactive Scope Model - a new model integrating homeostasis, allostasis, and stress. Horm Behav. 2009;55(3):375-89. Epub 2009/05/28. doi: 10.1016/j.yhbeh.2008.12.009. PubMed PMID: 19470371.
2. Levine S, Ursin H. What is stress? Neurobiology and Neuroendocrinology: New York: Marcel Dekker; 1991.
3. Del Giudice M, Buck CL, Chaby LE, Gormally BM, Taff CC, Thawley CJ, et al. What Is Stress? A Systems Perspective. Integr Comp Biol. 2018;58(6):1019-32. Epub 2018/09/12. doi: 10.1093/icb/icy114. PubMed PMID: 30204874.
4. Du Preez A, Law T, Onorato D, Lim YM, Eiben P, Musaelyan K, et al. The type of stress matters: repeated injection and permanent social isolation stress in male mice have a differential effect on anxiety- and depressive-like behaviours, and associated biological alterations. Transl Psychiatry. 2020;10(1):325. Epub 2020/09/23. doi: 10.1038/s41398-020-01000-3. PubMed PMID: 32958745; PubMed Central PMCID: PMCPMC7505042.
5. Du Preez A, Eum J, Eiben I, Eiben P, Zunszain PA, Pariante CM, et al. Do different types of stress differentially alter behavioural and neurobiological outcomes associated with depression in rodent models? A systematic review. Front Neuroendocrinol. 2021;61:100896. Epub 2020/12/29. doi: 10.1016/j.yfrne.2020.100896. PubMed PMID: 33359461.
6. Barnum CJ, Pace TW, Hu F, Neigh GN, Tansey MG. Psychological stress in adolescent and adult mice increases neuroinflammation and attenuates the response to LPS challenge. Journal of Neuroinflammation. 2012;9:1-15.
7. Liu X, Wu R, Tai F, Ma L, Wei B, Yang X, et al. Effects of group housing on stress induced emotional and neuroendocrine alterations. Brain Res. 2013;1502:71-80. Epub 2013/02/06. doi: 10.1016/j.brainres.2013.01.044. PubMed PMID: 23380532.
8. Pearson-Leary J, Zhao C, Bittinger K, Eacret D, Luz S, Vigderman AS, et al. The gut microbiome regulates the increases in depressive-type behaviors and in inflammatory processes in the ventral hippocampus of stress vulnerable rats. Mol Psychiatry. 2020;25(5):1068-79. Epub 2019/03/06. doi: 10.1038/s41380-019-0380-x. PubMed PMID: 30833676.
9. Davis DJ, Doerr HM, Grzelak AK, Busi SB, Jasarevic E, Ericsson AC, et al. Lactobacillus plantarum attenuates anxiety-related behavior and protects against stress-induced dysbiosis in adult zebrafish. Sci Rep. 2016;6:33726. Epub 2016/09/20. doi: 10.1038/srep33726. PubMed PMID: 27641717; PubMed Central PMCID: PMCPMC5027381.
10. Chevalier G, Siopi E, Guenin-Mace L, Pascal M, Laval T, Rifflet A, et al. Effect of gut microbiota on depressive-like behaviors in mice is mediated by the endocannabinoid system. Nat Commun. 2020;11(1):6363. Epub 2020/12/15. doi: 10.1038/s41467-020-19931-2. PubMed PMID: 33311466; PubMed Central PMCID: PMCPMC7732982.
11. Ritz NL, Brocka M, Butler MI, Cowan CS, Barrera-Bugueño C, Turkington CJ, et al. Social anxiety disorder-associated gut microbiota increases social fear. Proceedings of the National Academy of Sciences. 2023;121(1):e2308706120.
12. de Weerth C. Do bacteria shape our development? Crosstalk between intestinal microbiota and HPA axis. Neurosci Biobehav Rev. 2017;83:458-71. Epub 2017/09/18. doi: 10.1016/j.neubiorev.2017.09.016. PubMed PMID: 28918360.
13. Mir HD, Milman A, Monnoye M, Douard V, Philippe C, Aubert A, et al. The gut microbiota metabolite indole increases emotional responses and adrenal medulla activity in chronically stressed male mice. Psychoneuroendocrinology. 2020;119:104750. Epub 2020/06/23. doi: 10.1016/j.psyneuen.2020.104750. PubMed PMID: 32569990.
14. Agranyoni O, Meninger-Mordechay S, Uzan A, Ziv O, Salmon-Divon M, Rodin D, et al. Gut microbiota determines the social behavior of mice and induces metabolic and inflammatory

changes in their adipose tissue. NPJ Biofilms Microbiomes. 2021;7(1):28. Epub 2021/03/21. doi: 10.1038/s41522-021-00193-9. PubMed PMID: 33741982.
15. Werbner M, Barsheshet Y, Werbner N, Zigdon M, Averbuch I, Ziv O, et al. Social-Stress-Responsive Microbiota Induces Stimulation of Self-Reactive Effector T Helper Cells. mSystems. 2019;4(4). Epub 2019/05/18. doi: 10.1128/mSystems.00292-18. PubMed PMID: 31098398; PubMed Central PMCID: PMCPMC6517692.
16. Weiss S. Microbiota as mediator and moderator of stress. Bioessays. 2021;43(1):e2000277. Epub 2020/11/26. doi: 10.1002/bies.202000277. PubMed PMID: 33236390.
17. Moeller AH, Sanders JG. Roles of the gut microbiota in the adaptive evolution of mammalian species. Philos Trans R Soc Lond B Biol Sci. 2020;375(1808):20190597. Epub 2020/08/11. doi: 10.1098/rstb.2019.0597. PubMed PMID: 32772670; PubMed Central PMCID: PMCPMC7435157.
18. Candela M, Biagi E, Maccaferri S, Turroni S, Brigidi P. Intestinal microbiota is a plastic factor responding to environmental changes. Trends in microbiology. 2012;20(8):385-91.
19. David LA, Materna AC, Friedman J, Campos-Baptista MI, Blackburn MC, Perrotta A, et al. Host lifestyle affects human microbiota on daily timescales. Genome biology. 2014;15(7):1-15.
20. David LA, Maurice CF, Carmody RN, Gootenberg DB, Button JE, Wolfe BE, et al. Diet rapidly and reproducibly alters the human gut microbiome. Nature. 2014;505(7484):559-63.
21. Turnbaugh PJ, Ridaura VK, Faith JJ, Rey FE, Knight R, Gordon JI. The effect of diet on the human gut microbiome: a metagenomic analysis in humanized gnotobiotic mice. Science translational medicine. 2009;1(6):6ra14-6ra.
22. Huang L, Duan C, Xia X, Wang H, Wang Y, Zhong Z, et al. Commensal microbe-derived propionic acid mediates juvenile social isolation-induced social deficits and anxiety-like behaviors. Brain Research Bulletin. 2021;166:161-71.
23. Usui N, Matsuzaki H, Shimada S. Characterization of Early Life Stress-Affected Gut Microbiota. Brain sciences. 2021;11(7):913.
24. Dunphy-Doherty F, O'Mahony SM, Peterson VL, O'Sullivan O, Crispie F, Cotter PD, et al. Post-weaning social isolation of rats leads to long-term disruption of the gut microbiota-immune-brain axis. Brain, behavior, and immunity. 2018;68:261-73.
25. Siopi E, Chevalier G, Katsimpardi L, Saha S, Bigot M, Moigneu C, et al. Changes in gut microbiota by chronic stress impair the efficacy of fluoxetine. Cell Reports. 2020;30(11):3682-90. e6.
26. Wang P, Wu PF, Wang HJ, Liao F, Wang F, Chen JG. Gut microbiome-derived ammonia modulates stress vulnerability in the host. Nat Metab. 2023;5(11):1986-2001. Epub 2023/10/24. doi: 10.1038/s42255-023-00909-5. PubMed PMID: 37872351.
27. Ritz NL, Draper LA, Bastiaanssen TF, Turkington CJ, Peterson VL, van de Wouw M, et al. The gut virome is associated with stress-induced changes in behaviour and immune responses in mice. Nature Microbiology. 2024;9(2):359-76.
28. Apfelbach R, Blanchard CD, Blanchard RJ, Hayes RA, McGregor IS. The effects of predator odors in mammalian prey species: a review of field and laboratory studies. Neuroscience & Biobehavioral Reviews. 2005;29(8):1123-44.
29. Baumbach JL, Mui CY, Zahra FT, Martin LJ. A single exposure to the predator odor 2, 4, 5-trimethylthiazoline causes long-lasting affective behavioral changes in female mice: Modulation by kappa opioid receptor signaling. Pharmacology Biochemistry and Behavior. 2024;242:173822.

30. Post RJ, Dahlborg KM, O'Loughlin LE, Bloom CM. Effects of juvenile exposure to predator odor on adolescent and adult anxiety and pain nociception. Physiology & behavior. 2014;131:57-61.
31. Hebb AL, Zacharko RM, Gauthier M, Trudel F, Laforest S, Drolet G. Brief exposure to predator odor and resultant anxiety enhances mesocorticolimbic activity and enkephalin expression in CD-1 mice. European Journal of Neuroscience. 2004;20(9):2415-29.
32. Janitzky K, Stork O, Lux A, Yanagawa Y, Schwegler H, Linke R. Behavioral effects and pattern of brain c-fos mRNA induced by 2, 5-dihydro-2, 4, 5-trimethylthiazoline, a component of fox feces odor in GAD67-GFP knock-in C57BL/6 mice. Behavioural brain research. 2009;202(2):218-24.
33. Hebb AL, Zacharko RM, Dominguez H, Trudel F, Laforest S, Drolet G. Odor-induced variation in anxiety-like behavior in mice is associated with discrete and differential effects on mesocorticolimbic cholecystokinin mRNA expression. Neuropsychopharmacology. 2002;27(5):744-55.
34. Oh JH, Rehermann B. Natural versus laboratory world: incorporating wild-derived microbiota into preclinical rodent models. The Journal of Immunology. 2021;207(7):1703-9.
35. Bruno P, Schüler T, Rosshart SP. Born to be wild: utilizing natural microbiota for reliable biomedical research. Trends in Immunology. 2024.
36. Sheehan MJ, Campbell P, Miller CH. Evolutionary patterns of major urinary protein scent signals in house mice and relatives. Molecular ecology. 2019;28(15):3587-601.
37. Miller CH, Hillock MF, Yang J, Carlson-Clarke B, Haxhillari K, Lee AY, et al. Dynamic changes to signal allocation rules in response to variable social environments in house mice. Communications Biology. 2023;6(1):297.
38. Miller CH, Haxhillari K, Hillock MF, Reichard TM, Sheehan MJ. Scent mark signal investment predicts fight dynamics in house mice. Proceedings of the Royal Society B. 2023;290(1993):20222489.
39. Gould TD, Dao DT, Kovacsics CE. The open field test. Mood and anxiety related phenotypes in mice. 2009:1-20.
40. Hacquemand R, Choffat N, Jacquot L, Brand G. Comparison between low doses of TMT and cat odor exposure in anxiety-and fear-related behaviors in mice. Behavioural brain research. 2013;238:227-31.
41. Blanchard RJ, Blanchard DC, Rodgers J, Weiss SM. The characterization and modelling of antipredator defensive behavior. Neuroscience & Biobehavioral Reviews. 1990;14(4):463-72.
42. Nollet M, Guisquet AML, Belzung C. Models of depression: unpredictable chronic mild stress in mice. Current protocols in pharmacology. 2013;61(1):5.65. 1-5.. 17.
43. Zangrossi Jr H, File SE. Behavioral consequences in animal tests of anxiety and exploration of exposure to cat odor. Brain research bulletin. 1992;29(3-4):381-8.
44. Rein B, Ma K, Yan Z. A standardized social preference protocol for measuring social deficits in mouse models of autism. Nat Protoc. 2020;15(10):3464-77. Epub 2020/09/09. doi: 10.1038/s41596-020-0382-9. PubMed PMID: 32895524; PubMed Central PMCID: PMCPMC8103520.
45. Liu J, Guo M, Zhang D, Cheng SY, Liu M, Ding J, et al. Adiponectin is critical in determining susceptibility to depressive behaviors and has antidepressant-like activity. Proc Natl Acad Sci U S A. 2012;109(30):12248-53. Epub 2012/07/11. doi: 10.1073/pnas.1202835109. PubMed PMID: 22778410; PubMed Central PMCID: PMCPMC3409774.
46. Grant RW, Dixit VD. Adipose tissue as an immunological organ. Obesity. 2015;23(3):512-8.
47. Wu Y, Ma Y. CCL2-CCR2 signaling axis in obesity and metabolic diseases. Journal of Cellular Physiology. 2024;239(4):e31192.

48. Kelly JR, Kennedy PJ, Cryan JF, Dinan TG, Clarke G, Hyland NP. Breaking down the barriers: the gut microbiome, intestinal permeability and stress-related psychiatric disorders. Frontiers in cellular neuroscience. 2015;9:392.
49. Bertin B, Desreumaux P, Dubuquoy L. Obesity, visceral fat and Crohn's disease. Current Opinion in Clinical Nutrition & Metabolic Care. 2010;13(5):574-80.
50. Karrasch T, Schaeffler A. Adipokines and the role of visceral adipose tissue in inflammatory bowel disease. Annals of Gastroenterology: Quarterly Publication of the Hellenic Society of Gastroenterology. 2016;29(4):424.
51. Batra A, Heimesaat M, Bereswill S, Fischer A, Glauben R, Kunkel D, et al. Mesenteric fat—control site for bacterial translocation in colitis? Mucosal Immunology. 2012;5(5):580-91.
52. Zhang L-j, Guerrero-Juarez CF, Hata T, Bapat SP, Ramos R, Plikus MV, et al. Dermal adipocytes protect against invasive Staphylococcus aureus skin infection. Science. 2015;347(6217):67-71.
53. Alcorn JF, Kolls JK. Killer fat. Science. 2015;347(6217):26-7.
54. Guo D-H, Yamamoto M, Hernandez CM, Khodadadi H, Baban B, Stranahan AM. Visceral adipose NLRP3 impairs cognition in obesity via IL-1R1 on CX3CR1+ cells. The Journal of clinical investigation. 2020;130(4):1961-76.
55. Sanders JG, Sprockett DD, Li Y, Mjungu D, Lonsdorf EV, Ndjango JN, et al. Widespread extinctions of co-diversified primate gut bacterial symbionts from humans. Nat Microbiol. 2023;8(6):1039-50. Epub 2023/05/12. doi: 10.1038/s41564-023-01388-w. PubMed PMID: 37169918; PubMed Central PMCID: PMCPMC10860671.
56. Parks DH, Chuvochina M, Rinke C, Mussig AJ, Chaumeil P-A, Hugenholtz P. GTDB: an ongoing census of bacterial and archaeal diversity through a phylogenetically consistent, rank normalized and complete genome-based taxonomy. Nucleic acids research. 2022;50(D1):D785-D94.
57. Chaumeil P-A, Mussig AJ, Hugenholtz P, Parks DH. GTDB-Tk: a toolkit to classify genomes with the Genome Taxonomy Database. Oxford University Press; 2020.
58. Olm MR, Crits-Christoph A, Bouma-Gregson K, Firek BA, Morowitz MJ, Banfield JF. inStrain profiles population microdiversity from metagenomic data and sensitively detects shared microbial strains. Nat Biotechnol. 2021. Epub 2021/01/20. doi: 10.1038/s41587-020-00797-0. PubMed PMID: 33462508.
59. Patel KV, Hunt AB, Castillo-Fernandez J, Abrams C, King T, Watson P, et al. Impact of acute stress on the canine gut microbiota. Scientific Reports. 2024;14(1):18897.
60. Rodiño-Janeiro BK, Khannous-Lleiffe O, Pigrau M, Willis JR, Salvo-Romero E, Nieto A, et al. Acute stress triggers sex-dependent rapid alterations in the human small intestine microbiota composition. Frontiers in Microbiology. 2025;15:1441126.
61. Bowen MT, Keats K, Kendig MD, Cakic V, Callaghan PD, McGregor IS. Aggregation in quads but not pairs of rats exposed to cat odor or bright light. Behavioural processes. 2012;90(3):331-6.
62. Sandi C, Haller J. Stress and the social brain: behavioural effects and neurobiological mechanisms. Nature reviews neuroscience. 2015;16(5):290-304.
63. Li A-l, Ni W-w, Li Y, Zhang X, Yang J-j, Ma X-y, et al. Effect of 2′-fucosyllactose supplementation on intestinal flora in mice with intestinal inflammatory diseases. International Dairy Journal. 2020;110:104797.
64. Zhao R, Shen GX. Impact of anthocyanin component and metabolite of Saskatoon berry on gut microbiome and relationship with fecal short chain fatty acids in diet-induced insulin resistant mice. The Journal of Nutritional Biochemistry. 2023;111:109201.

65. Zhan F, Song W, Fan Y, Wang F, Wang Q. Cucurbitacin E Alleviates Colonic Barrier Function Impairment and Inflammation Response and Improves Microbial Composition on Experimental Colitis Models. Journal of Inflammation Research. 2024:2745-56.
66. Lee KS, Palatinszky M, Pereira FC, Nguyen J, Fernandez VI, Mueller AJ, et al. An automated Raman-based platform for the sorting of live cells by functional properties. Nature microbiology. 2019;4(6):1035-48.
67. Volk JK, Nyström EE, van der Post S, Abad BM, Schroeder BO, Johansson Å, et al. The Nlrp6 inflammasome is not required for baseline colonic inner mucus layer formation or function. Journal of Experimental Medicine. 2019;216(11):2602-18.
68. van der Hee B, Wells JM. Microbial regulation of host physiology by short-chain fatty acids. Trends in microbiology. 2021;29(8):700-12.
69. Zhu Y, Chen B, Zhang X, Akbar MT, Wu T, Zhang Y, et al. Exploration of the muribaculaceae family in the gut microbiota: diversity, metabolism, and function. Nutrients. 2024;16(16):2660.
70. Agirman G, Yu KB, Hsiao EY. Signaling inflammation across the gut-brain axis. Science. 2021;374(6571):1087-92.
71. Fung TC. The microbiota-immune axis as a central mediator of gut-brain communication. Neurobiology of disease. 2020;136:104714.
72. Puricelli C, Rolla R, Gigliotti L, Boggio E, Beltrami E, Dianzani U, et al. The gut-brain-immune axis in autism spectrum disorders: a state-of-art report. Frontiers in Psychiatry. 2022;12:755171.
73. Crumeyrolle-Arias M, Jaglin M, Bruneau A, Vancassel S, Cardona A, Dauge V, et al. Absence of the gut microbiota enhances anxiety-like behavior and neuroendocrine response to acute stress in rats. Psychoneuroendocrinology. 2014;42:207-17. Epub 2014/03/19. doi: 10.1016/j.psyneuen.2014.01.014. PubMed PMID: 24636517.
74. Lyte JM, Gheorghe CE, Goodson MS, Kelley-Loughnane N, Dinan TG, Cryan JF, et al. Gut-brain axis serotonergic responses to acute stress exposure are microbiome-dependent. Neurogastroenterol Motil. 2020;32(11):e13881. Epub 2020/05/12. doi: 10.1111/nmo.13881. PubMed PMID: 32391630.
75. Rosell-Cardona C, Collins MK, O'Riordan KJ, Goodson MS, Kelley-Loughnane N, Cryan JF, et al. Acute stress enhances synaptic plasticity in male mice via a microbiota-dependent mechanism. Neuropharmacology. 2025;273:110434.
76. Vagnerová K, Vodička M, Hermanová P, Ergang P, Šrůtková D, Klusoňová P, et al. Interactions between gut microbiota and acute restraint stress in peripheral structures of the hypothalamic–pituitary–adrenal axis and the intestine of male mice. Frontiers in immunology. 2019;10:2655.
77. Moeller AH, Suzuki TA, Phifer-Rixey M, Nachman MW. Transmission modes of the mammalian gut microbiota. Science. 2018;362(6413):453-7. Epub 2018/10/27. doi: 10.1126/science.aat7164. PubMed PMID: 30361372.
78. Vogt CC, Zipple MN, Sprockett DD, Miller CH, Hardy SX, Arthur MK, et al. Female behavior drives the formation of distinct social structures in C57BL/6J versus wild-derived outbred mice in field enclosures. BMC biology. 2024;22(1):35.
79. Tuttle AH, Tansley S, Dossett K, Tohyama S, Khoutorsky A, Maldonado-Bouchard S, et al. Social propinquity in rodents as measured by tube cooccupancy differs between inbred and outbred genotypes. Proceedings of the National Academy of Sciences. 2017;114(21):5515-20.
80. Smith J, Hurst JL, Barnard C. Comparing behaviour in wild and laboratory strains of the house mouse: levels of comparison and functional inference. Behavioural processes. 1994;32(1):79-86.

81. Moy S, Nadler J, Perez A, Barbaro R, Johns J, Magnuson T, et al. Sociability and preference for social novelty in five inbred strains: an approach to assess autistic-like behavior in mice. Genes, Brain and Behavior. 2004;3(5):287-302.
82. Blanchard RJ, Hebert MA, Ferrari P, Palanza P, Figueira R, Blanchard DC, et al. Defensive behaviors in wild and laboratory (Swiss) mice: the mouse defense test battery. Physiology & behavior. 1998;65(2):201-9.
83. Dumont BL, Gatti DM, Ballinger MA, Lin D, Phifer-Rixey M, Sheehan MJ, et al. Into the Wild: A novel wild-derived inbred strain resource expands the genomic and phenotypic diversity of laboratory mouse models. PLoS genetics. 2024;20(4):e1011228.
84. Rodriguez A, Zhang H, Klaminder J, Brodin T, Andersson PL, Andersson M. ToxTrac: a fast and robust software for tracking organisms. Methods in Ecology and Evolution. 2018;9(3):460-4.
85. Nollet M. Models of Depression: Unpredictable Chronic Mild Stress in Mice. Curr Protoc. 2021;1(8):e208. Epub 2021/08/19. doi: 10.1002/cpz1.208. PubMed PMID: 34406704.
86. Kalueff AV, Tuohimaa P. Grooming analysis algorithm for neurobehavioural stress research. Brain Research Protocols. 2004;13(3):151-8.
87. Andrews S. FastQC: a quality control tool for high throughput sequence data. Babraham Bioinformatics, Babraham Institute, Cambridge, United Kingdom; 2010.
88. Dobin A, Davis CA, Schlesinger F, Drenkow J, Zaleski C, Jha S, et al. STAR: ultrafast universal RNA-seq aligner. Bioinformatics. 2013;29(1):15-21.
89. Mölder F, Jablonski KP, Letcher B, Hall MB, Tomkins-Tinch CH, Sochat V, et al. Sustainable data analysis with Snakemake. F1000Research. 2021;10.
90. Martin M. Cutadapt removes adapter sequences from high-throughput sequencing reads. EMBnet journal. 2011;17(1):10-2.
91. Langmead B, Salzberg SL. Fast gapped-read alignment with Bowtie 2. Nature methods. 2012;9(4):357-9.
92. Li D, Liu C-M, Luo R, Sadakane K, Lam T-W. MEGAHIT: an ultra-fast single-node solution for large and complex metagenomics assembly via succinct de Bruijn graph. Bioinformatics. 2015;31(10):1674-6.
93. Gurevich A, Saveliev V, Vyahhi N, Tesler G. QUAST: quality assessment tool for genome assemblies. Bioinformatics. 2013;29(8):1072-5.
94. Brown CT, Irber L. sourmash: a library for MinHash sketching of DNA. Journal of open source software. 2016;1(5):27.
95. Li H. Minimap2: pairwise alignment for nucleotide sequences. Bioinformatics. 2018;34(18):3094-100.
96. Alneberg J, Bjarnason BS, de Bruijn I, Schirmer M, Quick J, Ijaz UZ, et al. Binning metagenomic contigs by coverage and composition. Nat Methods. 2014;11(11):1144-6. Epub 2014/09/15. doi: 10.1038/nmeth.3103. PubMed PMID: 25218180.
97. Kang DD, Li F, Kirton E, Thomas A, Egan R, An H, et al. MetaBAT 2: an adaptive binning algorithm for robust and efficient genome reconstruction from metagenome assemblies. PeerJ. 2019;7:e7359.
98. Wu YW, Simmons BA, Singer SW. MaxBin 2.0: an automated binning algorithm to recover genomes from multiple metagenomic datasets. Bioinformatics. 2016;32(4):605-7. Epub 2015/10/31. doi: 10.1093/bioinformatics/btv638. PubMed PMID: 26515820.
99. Sieber CM, Probst AJ, Sharrar A, Thomas BC, Hess M, Tringe SG, et al. Recovery of genomes from metagenomes via a dereplication, aggregation and scoring strategy. Nature microbiology. 2018;3(7):836-43.

100. Parks DH, Imelfort M, Skennerton CT, Hugenholtz P, Tyson GW. CheckM: assessing the quality of microbial genomes recovered from isolates, single cells, and metagenomes. Genome research. 2015;25(7):1043-55.
101. Orakov A, Fullam A, Coelho LP, Khedkar S, Szklarczyk D, Mende DR, et al. GUNC: detection of chimerism and contamination in prokaryotic genomes. Genome Biol. 2021;22(1):178. Epub 2021/06/15. doi: 10.1186/s13059-021-02393-0. PubMed PMID: 34120611; PubMed Central PMCID: PMCPMC8201837.
102. Olm MR, Brown CT, Brooks B, Banfield JF. dRep: a tool for fast and accurate genomic comparisons that enables improved genome recovery from metagenomes through de-replication. The ISME journal. 2017;11(12):2864-8.
103. McMurdie PJ, Holmes S. phyloseq: an R package for reproducible interactive analysis and graphics of microbiome census data. PloS one. 2013;8(4):e61217.
104. Kuznetsova A, Brockhoff P, Christensen R. Package 'lmertest'. Version 3.1-0. Computer software] Retrieved from https://cran r-project org. 2019.
105. Anderson MJ. Permutational multivariate analysis of variance. Department of Statistics, University of Auckland, Auckland. 2005;26:32-46.
106. Anderson MJ, Ellingsen KE, McArdle BH. Multivariate dispersion as a measure of beta diversity. Ecology letters. 2006;9(6):683-93.
107. Oksanen J, Blanchet FG, Kindt R, Legendre P, Minchin PR, O'hara R, et al. Package 'vegan'. Community ecology package, version. 2013;2(9):1-295.
108. Love MI, Huber W, Anders S. Moderated estimation of fold change and dispersion for RNA-seq data with DESeq2. Genome biology. 2014;15(12):1-21.
109. Stephens M. False discovery rates: a new deal. Biostatistics. 2017;18(2):275-94.
110. Yu G, Wang L-G, Han Y, He Q-Y. clusterProfiler: an R package for comparing biological themes among gene clusters. Omics: a journal of integrative biology. 2012;16(5):284-7.
111. Wu T, Hu E, Xu S, Chen M, Guo P, Dai Z, et al. clusterProfiler 4.0: A universal enrichment tool for interpreting omics data. The Innovation. 2021;2(3):100141.
112. Pedregosa F, Varoquaux G, Gramfort A, Michel V, Thirion B, Grisel O, et al. Scikit-learn: Machine learning in Python. the Journal of machine Learning research. 2011;12:2825-30.
113. Wickham H, Chang W, Wickham MH. Package 'ggplot2'. Create elegant data visualisations using the grammar of graphics Version. 2016;2(1):1-189.

Figures and Tables

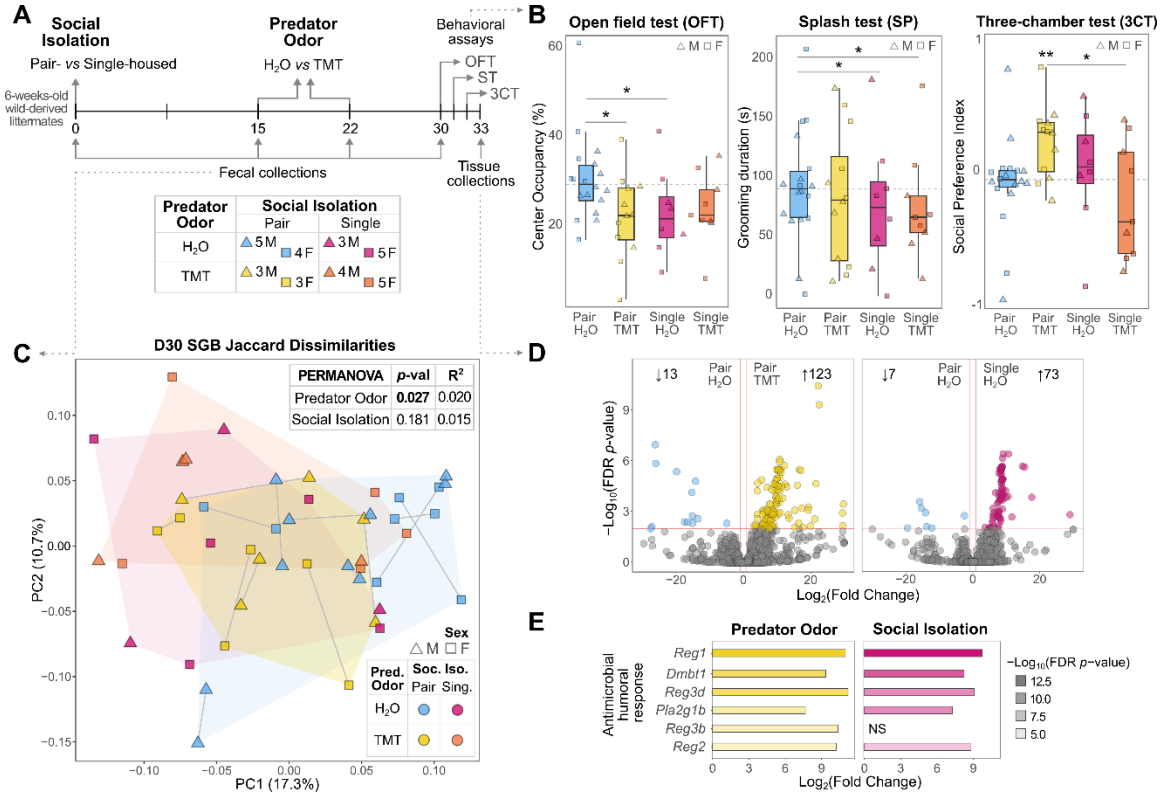

Figure 1. Brief predator-odor exposure altered host behavior, gene expression, and the gut microbiota. (**A**) The diagram shows the experiment timeline. Same-sex littermates of wild-derived mice (*Mus musculus domesticus*) were either pair or single-housed for approximately 30 days. Mice from both housing groups were exposed to either water (H_2O) or predator odor (TMT) for 15 minutes on days 15 and 22 of the experiment. Fecal samples for metagenomic analyses were collected on days 0, 15, 22, and 30. At the end of the experiment, mouse behavior was assayed over three consecutive days (OFT, open-field test; ST, splash test; 3CT, three-chamber test), after which, mice were sacrificed and their visceral adipose tissue (VAT) collected for transcriptomic analyses. The embedded table shows the number of male (triangles) and female (squares) replicate cages per treatment group. (**B**) Box plots show the amount of time that male (triangles) and female (squares) mice of different treatment groups spent occupying the central area of the open-field test (OFT), the time spent grooming after being sprayed with a 10% sucrose solution in the splash test (SP), and the social preference index measured during the three-chamber test (3CT). Differences between the groups were tested with a pairwise comparison of the marginal means from a linear mixed-effects model (LMM) accounting for sex, litter and cage effects (* = p-value < 0.05). In the 3CT plot, we also tested whether the social preference index within each group significantly differed from zero with a one-sample t-

test (** = *p*-value < 0.01). Dashed gray lines indicate the unstressed controls' mean. (**C**) Principal coordinate analysis (PCoA) shows the first two axes of the ordinated Jaccard dissimilarity matrix of species genome bins (SGBs) composition at the end of the experiment (D30). Points represent the species profiles of male (triangles) and female (squares) mice, colored by treatment group: blue, Pair H_2O; yellow, Pair TMT; pink, Single H_2O; orange, Single TMT. Pair-housed cage-mates are connected by a gray line. The percent variation in SGB composition explained by each axis is enclosed in parenthesis. (**D**) Volcano plots show the log2-transformed fold change (LFC) in the expression of genes (points) in the visceral adipose tissue (VAT) of male and female mice in response to predator-odor exposure (left) or social isolation (right). Genes in the upper-outer quadrants were differentially expressed (DEGs; absolute LFC > 1 and FDR-adjusted *p*-value < 0.01), and their total number is presented at the top of the plot. (**E**) Bar plots show the absolute LFC of genes belonging to the anti-microbial humoral response biological pathway, which was found to be significantly enriched in the DEGs of mice exposed to predator odor (left) and social isolation (right). Genes are ordered and colored by the $-\log_{10}$(FDR-adjusted *p*-value) resulting from the differential expression analysis. Gene *Reg3b* was not included in the social isolation plot as it was not differentially expressed.

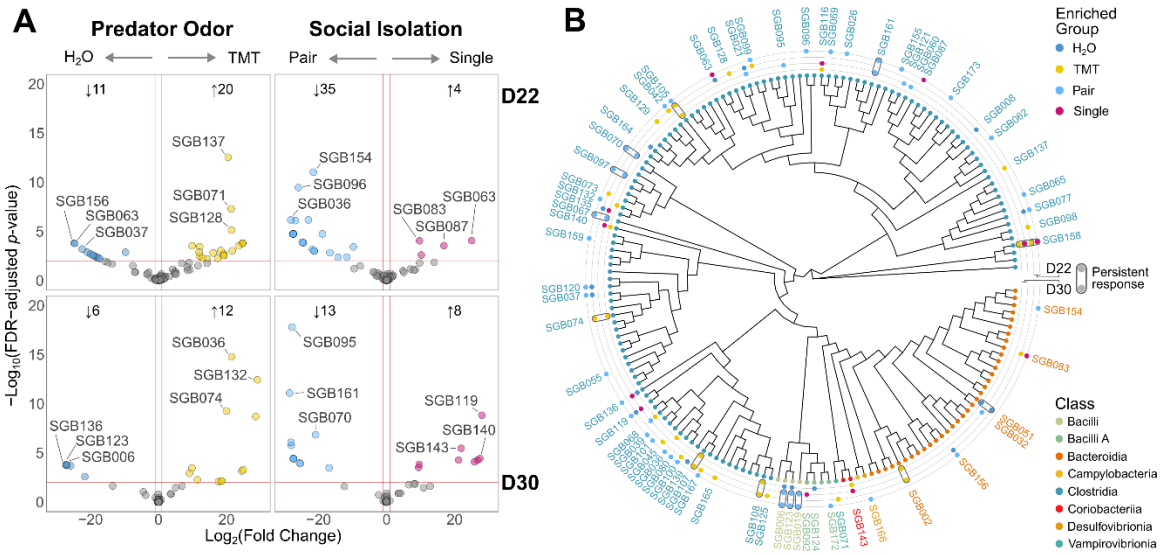

Figure 2. Predator-odor exposure drove persistent alterations in the relative abundances of specific SGBs. (**A**) Volcano plots show the $\log_2$-transformed fold change (LFC) in the relative abundances of species (points) in the gut microbiota of male and female mice in response to predator-odor exposure (left column) or social isolation (right column) a week after the first TMT exposure (D22; top row) and a week after the second TMT exposure (D30; bottom row). Upper-outer quadrants contain points corresponding to differentially abundant SGBs (DESeq2; absolute LFC > 1 and FDR-adjusted *p*-value < 0.01), whose total number is presented at the top of the plot. The three most significantly differentially abundant SGBs in each quadrant are labelled. (**B**) The phylogenetic tree shows the evolutionary relationship (number of amino acid substitutions) between representative SGBs in our custom database, with the tips colored by bacterial class. The rings show differentially abundant SGBs at D22 (outer two rings) and D30 (inner two rings), colored by the stressor group in which they were enriched: H_2O (dark blue) *vs.* TMT (yellow) and Pair (light blue) *vs.* Single (pink). SGBs that displayed a persistent response to the stressors across both D22 and D30 are encircled.

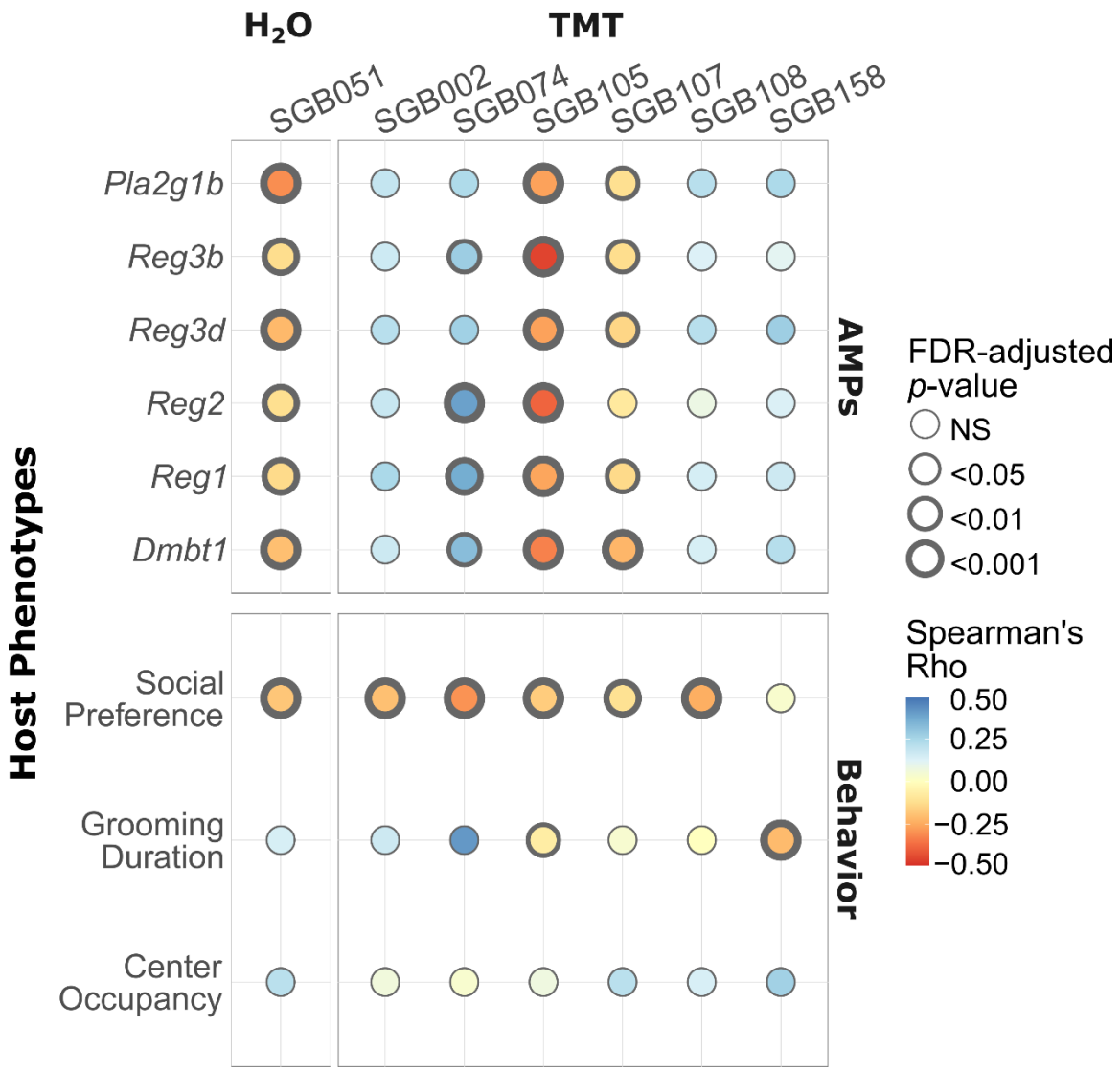

Figure 3. Predator odor–responsive SGBs co-varied with host anti-microbial and behavioral responses. (**A**) The correlation matrix shows associations between the D22 relative abundances of SGBs that were persistently associated with predator-odor exposure (differentially abundant at both D22 and D30) and host anti-microbial (AMPs) and behavioral responses. The color of the circles corresponds to Spearman's Rho from a partial correlation test that accounted for the effects of stressor treatments. These analyses tested whether variation in SGB abundances within treatment groups (Pair H_2O, Pair TMT, Single H_2O, Single TMT) was associated with within-group variation in behavior or AMP expression. The thickness of the circle border indicates the significance level of this same correlation test, corrected for multiple comparisons (FDR).

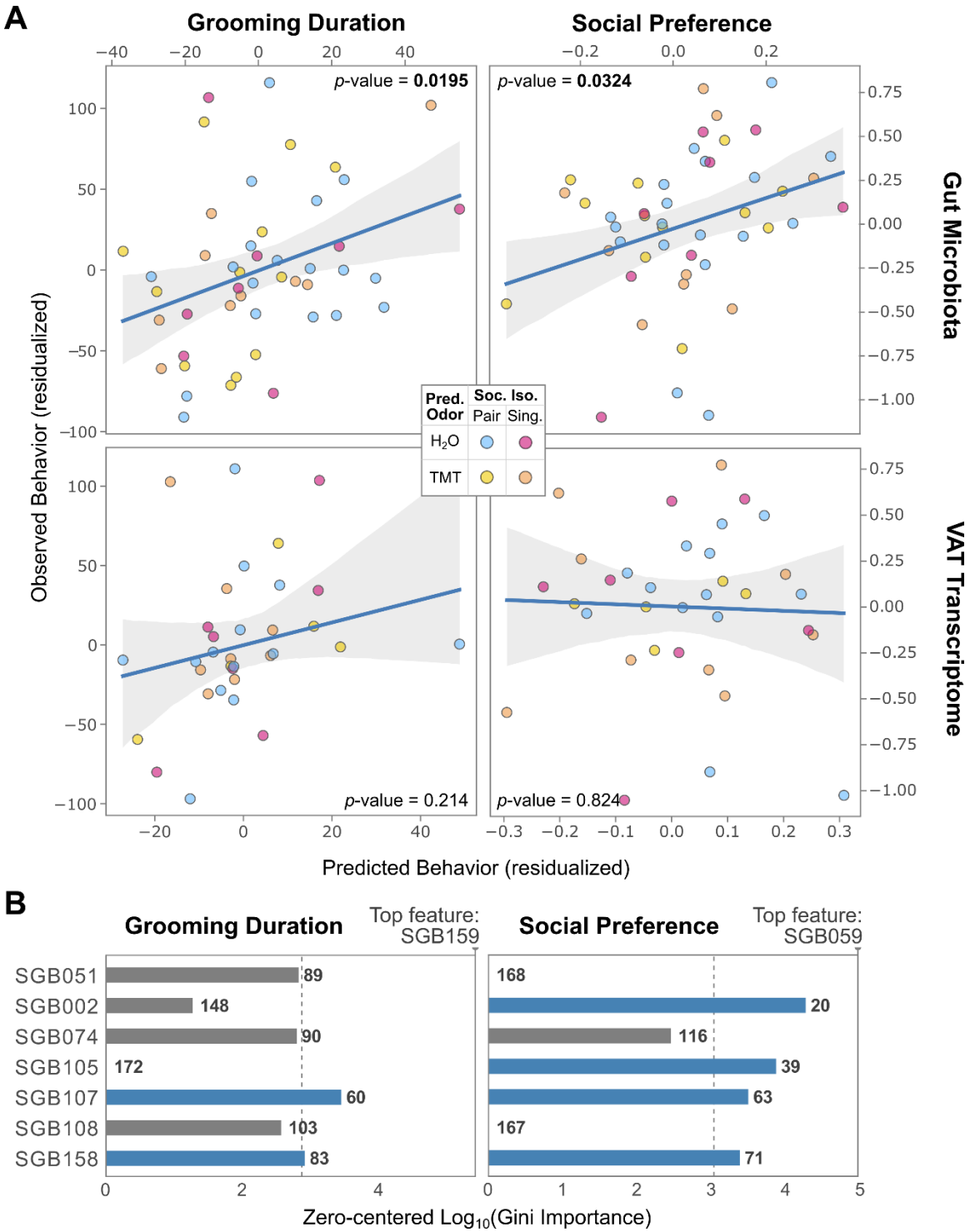

Figure 4. The gut microbiota was a better predictor of host behavior than was host gene expression. (**A**) The scatter plots show the relation between observed grooming (left column) and social (right column) behavior (residualized to account for the effect of stressor treatment) and the values predicted by a random forest model based on SGB

relative abundances at D30 (top row) or VAT gene expression (bottom row). Points are colored by treatment group: blue, Pair H_2O; yellow, Pair TMT; pink, Single H_2O; orange, Single TMT. The significance of the linear regression is shown in the upper inner corner, with significant values (p-value < 0.05) in bold. (**B**) The bar plots show the zero-centered $\log_{10}$(Gini Importance) of SGBs persistently associated with predator-odor exposure (differentially abundant at both D22 and D30) for predicting grooming (left) and social (right) behaviors. The SGB importance rank order is annotated in bold, and the bars are colored blue if the SGB was among the top half most important features (the dashed line indicates the median importance value). The maximum x-axis value corresponds to the most important SGB, identified in the top right corner.

Table 1. Effect of predator-odor exposure (PO) and social isolation (SI) on species-level genome bins (SGB) composition.[a]

Timepoint	Stressor	Jaccard		Bray-Curtis	
		***p*-value**	**R^2**	***p*-value**	**R^2**
D0	**PO**	0.691	0.013	0.122	0.016
	SI	0.622	0.013	0.180	0.014
D15	**PO**	0.384	0.020	0.285	0.010
	SI	0.990	0.010	0.590	0.007
D22	**PO**	0.540	0.017	0.106	0.018
	SI	0.140	0.023	**0.002**	0.029
D30	**PO**	**0.027**	0.020	**0.002**	0.026
	SI	0.181	0.015	0.208	0.011

[a] Significant results are **bolded** (p-value < 0.05).

Table 2. Taxonomic classification of SGBs that displayed a persistent response to predator-odor exposure (DA at both D22 and D30).

SGBs	Phylum	Class	Order	Family	Genus	Species
SGB051	Bacteroidota	Bacteroidia	Bacteroidales	*Muribaculaceae*	*Lepagella*	*Lepagella sp002361155*
SGB002	Bacteroidota	Bacteroidia	Bacteroidales	*Rikenellaceae*	*Alistipes*	*Alistipes sp910587675*
SGB074	Bacillota A	Clostridia	Oscillospirales	*Oscillospiraceae*	*Pelethomonas*	*Pelethomonas sp009774055*
SGB105	Bacillota A	Clostridia	Lachnospirales	*Lachnospiraceae*	*Acetatifactor*	*Acetatifactor sp011959105*
SGB107	Bacillota A	Clostridia	Christensenellales	*Borkfalkiaceae*	*Gallimonas*	*Gallimonas sp910585595*
SGB108	Bacillota A	Clostridia	Christensenellales	*Borkfalkiaceae*	*Coproplasma*	*Coproplasma sp910583855*
SGB158	Bacillota A	Clostridia	Lachnospirales	*Lachnospiraceae*	*CAG-303*	*CAG-303 sp910585215*